


## Article

# The Optimization of Canola Crop Production through Wheat Residue Management within a Western Canadian Context—A Case Study of Saint-Front, Saskatchewan

Xiaying Xin <sup>1,2</sup>, Guohe Huang <sup>2,\*</sup>, David Halstead <sup>3</sup>, Katelyn Gaetz <sup>4</sup>, Leila Benmerrouche <sup>3</sup>, Jing Huang <sup>2</sup>, Yuwei Wu <sup>2</sup>, Jinbo Zhang <sup>5</sup> , Yupeng Fu <sup>2</sup> and Nan Wang <sup>2</sup>

<sup>1</sup> State Key Laboratory of Marine Pollution (SKLMP), School of Energy and Environment, City University of Hong Kong, Kowloon, Hong Kong SAR, China; xiayixin@cityu.edu.hk

<sup>2</sup> Institute for Energy, Environment and Sustainable Communities, University of Regina, Regina, SK S4S 0A2, Canada; jhbamboo@outlook.com (J.H.); yuwei930822@gmail.com (Y.W.); yfz423@uregina.ca (Y.F.); nanwang9305@163.com (N.W.)

<sup>3</sup> Saskatchewan Polytechnic, Prince Albert, SK S6V 7S4, Canada; HALSTEAD@saskpolytech.ca (D.H.); Lei.leis.123@gmail.com (L.B.)

<sup>4</sup> Prairie Agricultural Machinery Institute, Humboldt, SK S0K 2A0, Canada; kgaetz@pami.ca

<sup>5</sup> College of Environmental Science and Engineering, Peking University, Beijing 100871, China; KimballZhang@outlook.com

\* Correspondence: huangg@uregina.ca



**Citation:** Xin, X.; Huang, G.; Halstead, D.; Gaetz, K.; Benmerrouche, L.; Huang, J.; Wu, Y.; Zhang, J.; Fu, Y.; Wang, N. The Optimization of Canola Crop Production through Wheat Residue Management within a Western Canadian Context—A Case Study of Saint-Front, Saskatchewan. *Sustainability* **2021**, *13*, 10459. <https://doi.org/10.3390/su131810459>

Academic Editor: Hamid Rezaei

Received: 24 August 2021

Accepted: 17 September 2021

Published: 20 September 2021

**Publisher's Note:** MDPI stays neutral with regard to jurisdictional claims in published maps and institutional affiliations.



**Copyright:** © 2021 by the authors. Licensee MDPI, Basel, Switzerland. This article is an open access article distributed under the terms and conditions of the Creative Commons Attribution (CC BY) license (<https://creativecommons.org/licenses/by/4.0/>).

**Abstract:** In this study, the processes of wheat residue degradation in combination with various tillage treatments were explored to determine the ideal management prescription for maximizing canola crop production. A field experiment within a western Canadian context (near Saint-Front, Saskatchewan), consisting of a 2 × 3 factorial design, was conducted to determine the fate of crop residue under different harvest and treatment scenarios. ATR-Fourier transform infrared (FTIR) spectroscopy, FTIR spectromicroscopy, and synchrotron-based X-ray fluorescence imaging (SR-XFI) were used to explore wheat residue degradation mechanisms. The results indicated maximum canola yields and residue degradation occurred in combination with a combine outfitted with an aftermarket chopper and post-harvest treatment by harrow. Crop residue degradation was attributed to cellulose/linen hydrolysis and supramolecular structure changes from high crystalline to amorphous cellulose. Multi-element loss usually accompanied crop residue degradation. An important aspect of this study is the adoption of field-scale analysis to accurately portray real-world sustainable management techniques within a western Canadian context. The findings provided an optimal combination of crop residue treatment and tillage treatment to increase canola production, which had the potential ability to be applied in other countries. It is also an initial attempt to develop a technical composite of FTIR spectromicroscopy and SR-XFI for examining the mechanism of residue decomposition.

**Keywords:** crop residue management; residue degradation; factorial design; ATR-FTIR spectroscopy; FTIR spectromicroscopy; synchrotron-based X-ray fluorescence imaging

## 1. Introduction

Crop residue management (CRM) is defined as leaving last season's crop residues on the soil surface after harvest; before and during the next planting, these residues provide cover for the soil [1]. Crop residues after proper treatments can be sources of nutrients for successful crops and improved soil, water, and air quality [2]. In a crop rotation system, crop residue produces substantial long-term benefits that likely outweigh any short-term gains associated with post-harvest tillage practices [3]. Managing crop residues in agriculture can be economically beneficial to producers and environmentally important to society [4]. CRM can provide protection against wind- and rain-affected soil erosion, increase organic

matter in the soil, maintain soil moisture, and improve infiltration, aeration, and tilth, to increase crop production [5].

Tillage is agricultural soil treatment by mechanical agitation of various types, such as digging, stirring, and overturning [6]. Tillage and planting strategies involving a soil surface cover of crop residue have been demonstrated to reduce soil losses [7]. Primary tillage can decompose crop residue and soil organic matter through enhanced aeration and the promotion of microbial activity in the soil [8]. However, primary tillage practices can be costly and can have negative short-term and long-term impacts on the physical, chemical, and biological properties of the soil [9]. Secondary tillage is performed after primary tillage to create proper soil tilth for seeding and planting. These operations do not cause much soil inversion and soil shifting from one place to another. Harrowing is a secondary tillage practice, with less power consumption compared to primary tillage. Harrowing can smooth soil surface, reduce aggregate size, and chop crop residues to facilitate their breakdown [10].

Crop residue consists of cellulose, lignin, hemicellulose, and various plant nutrients. Many biochemical processes occur during crop residue breakdown. These processes are influenced by soil and environmental conditions, including soil moisture and temperature, oxygen, pH, and microbial community [11]. CRM and tillage treatments can influence the size of the residue and the extent of contact it has with the soil, which in turn affects the rate of decomposition [12]. Roldán [13] performed a field test with seven treatments with various soil management methods to evaluate the effects of no tillage in combination with surface residue cover on maize cropping. The results indicated no-till management with 33% crop residue coverage improved soil quality characteristics when compared with conventional tillage operations. Chávez-Romero [14] investigated the effects of CRM, tillage, and fertilizer application on the degradation of plant residue. Tillage and crop residue cover management helped determine residue bacterial populations, wheat plant residue breakdown, and soil organic carbon concentrations. Crop and soil management practices affect the rate of residue breakdown and crop yields.

Fourier transform infrared spectroscopy (FTIR) has been used to analyze residue decomposition [15–17]. FTIR is a vibrational spectroscopic method, where the specimen is irradiated with infrared (IR) light [18]. IR spectra are obtained when molecules absorb specific frequencies of IR light. Attenuated total reflectance (ATR) FTIR can be applied as a non-destructive method [19]; it is sensitive to the structural changes in residue and therefore allows analysis of the degradation processes over time [20]. Kavkler [21] used FTIR and Raman spectroscopy to qualitatively analyze structural changes in cellulosic fibers. Bonnin [22] applied FTIR to obtain information on the conformational changes of wheat germ agglutinin and N-acetylglucosamine residues. However, techniques capable of imaging structural changes on residues and directly observing varied microelement distribution during residue decomposition are still not applicable. Fourier transform infrared (FTIR) spectromicroscopy and synchrotron-based X-ray fluorescence imaging (SR-XFI) may enable the development of images for main component changes and microelement distributions. However, they have not been associated with the evaluation of CRM and tillage practices.

Considering the Canadian contribution to the global canola market [23], it is necessary to optimize and increase Canadian canola crop production to reduce its management risk [24,25]. CRM can be applied to help optimize canola production. The objective of the current study is to optimize canola production through different residue management systems on a high-residue wheat crop and a subsequent canola crop within a western Canadian context. Such decomposition is evaluated in the context of two harvester-chopper combinations and three post-harvest treatments, consisting of tillage, no-till, and harrow treatments. It is hypothesized that harrow treatments could be optimal. FTIR spectromicroscopy and SR-XFI are presented to explore the mechanism of crop residue degradation. It is also hypothesized that FTIR could help reveal the crop residue degradation level. This study seeks to accurately represent real-world management techniques by combining

CRM and tillage practices within a field-scale analysis. The findings will be beneficial to Canadian agricultural and industrial sectors. It is also an initial attempt to develop a technical composite of FTIR imaging and SR-XFI for examining the mechanism of residue decomposition.

## 2. Materials and Methods

### 2.1. Area of Interest

A field was selected near Saint-Front, Saskatchewan, approximately 20 km east of the town of Spalding (LSD SE 10-39-16-W2, RM 368). The field was mostly open, with some lowland and brush around. Figure 1 illustrates the research plot, and harvest and post-harvest treatment areas are labeled. Four replications of each treatment were performed.



**Figure 1.** 2018–2019 treatment layout at Saint-Front, Saskatchewan.

### 2.2. Experimental Design and Wheat Harvest

The present experiment was based on a one-year field trial in a three-year project by the Prairie Agricultural Machinery Institute (PAMI). Wheat harvest occurred on 18 October 2018. A  $2 \times 3$  factorial design was used to harvest the field with each combine to carry out different treatments [26]. The design was used to select the optimal treatment combination for one-year data based on canola yields and crop residue degradation rate. Crop residue treatments were carried out by an OEM chopper and aftermarket chopper, being considered as model variables that are not parametric. Based on the cooperator's machinery, two separate combines were applied to complete the OEM chopper portion (Machine 1: Case IH 8120, Case factory internal chopper with stationary knife bank engaged, Case factory

spreader, 36 ft (14.6 m) Honeybee header; Machine 2: Case IH 8230, Case magnacut chopper with stationary knife bank engaged, Case factory spreader, 36 ft (14.6 m) Honeybee header), while Redhead Equipment used a combine for the aftermarket chopper treatments (Case IH 8240, Case factory internal chopper, Redekop MAV 4 row external chopper/spreader with stationary knife bank engaged, 35 ft (14.2 m) Macdon header).

Post-harvest treatments were carried out on 23 October 2018. Post-harvest management practices include harrow, tilled, and check, being considered as model variables that are not parametric. The heavy harrow treatments were performed using an 80 ft (24.4 m) model Degelman Strawmaster Pro harrow, featuring four rows of 5/8 in (1.6 cm)  $\times$  26 in (66 cm) harrow tines and hydraulic down pressure. Ground speed during the operation was 10 mph (16 km/h). Harrow direction changed based on the treatments, as the direction was chosen to make the harrow as efficient as possible (Figure S1). No noticeable difference was observed in the field with direction changes. Crop moisture and canola yield were analyzed by PAMI to help select an optimal treatment combination.

### 2.3. Sampling and Residue Organic Weight

The wheat straw residue was sampled 28 days and 56 days post-seeding. Each block was sampled with three replicates along a diagonal transect. Flight images were taken to show canola yielding at the same time (Figure S2). In the laboratory, residue sampled on day 56 was dried for 1 week at 35 °C and stored for sample testing. Sample batches of approximately 0.63 g residue were placed in crucibles (40 mm diameter, 38 mm depth), heated in a muffle oven (Nabertherm, P320, Bremen, Germany) at 600 °C for 6 h in an oxygen-limited environment, and cooled down to room temperature (23 °C) to a constant weight. Crucible weight and residue weight were recorded before and after drying.

### 2.4. Residue Degradation Analyses by ATR-FTIR

The spectra of residue samples were recorded with a Bruker TEMSOR 27 IR FTIR-ATR Spectrometer. All samples were freeze-dried and ground into powder. A total of 144 samples were sequentially placed on the diamond radiation area of the ATR Gordien Gate device. Spectral data were collected by the spectrometer, and the interferogram was converted by a Fourier transformation to yield an FTIR spectrum file. Each spectrum file consisted of an average of 64 scans in the 4000 to 550  $\text{cm}^{-1}$  spectral range, using the reflection mode with a resolution of 4  $\text{cm}^{-1}$ .

### 2.5. Imaging Degraded Residue Samples through FTIR Spectromicroscopy

FTIR spectromicroscopy was used to image the distribution of main functional groups in crop residue on beamline 01B1–01(MidIR) at the Canadian Light Source (CLS) [27]. A Bruker Vertex 70v interferometer coupled to a Hyperion 3000 IR confocal microscope was used to obtain the images using a globalar, a thermal light source (Figure S3) [28,29]. A 15 $\times$  objective was used. A dry nitrogen purge was applied to maintain samples by removing  $\text{CO}_2$  and  $\text{H}_2\text{O}$  interference [28,30]. Spectral maps were attained using a resolution of 4  $\text{cm}^{-1}$  in reflection mode. Each spectrum was an average of 64 scans, using a 64  $\times$  64 pixel mid-infrared FPA detector (Bruker Optics).

### 2.6. Imaging Elemental Distribution through SR-XFI

Micro XFI was used to map six elements—Br, Ca, Fe, Pb, Se, and As—at the VESPERs (very sensitive elemental and structural probe employing radiation from a synchrotron) beamline at the CLS. The storage ring of the CLS operated at an energy of 2.9 GeV and a current range of 250–150 mA [28]. The beamline consisted of a microprobe using hard X-rays in the energy range of 5–30 keV to irradiate a microvolume of samples. The beam spot size ranged from 2  $\times$  2 to 5  $\times$  5  $\mu\text{m}$ . Residue samples were scanned using a polychromatic (pink) beam with a spot size of 3  $\times$  3  $\mu\text{m}$  and a step size of 30  $\mu\text{m}$  with a dwell time of 5 s per data point. The samples were deposited on metal-free Lexan<sup>TM</sup> polycarbonate sheets and then mounted on a sample holder attaching to a motorized stage. The synchrotron



X-ray beam (pink) was oriented 90° to the sample. A Vortex<sup>®</sup> silicon drift detector (SDD), positioned 50 mm away from the sample at an angle of 45° to the incident beam, was used for simultaneous collection of the emitted X-ray fluorescence signals of tested elements. The map size of approximately 1490 µm × 1520 µm was selected for the elemental mapping.

### 2.7. Statistical Analysis

Quantitative data were reduced to the mean and standard deviation for the remaining analyses. At least three repeats were used for each measurement. The main effects of the different factors and their interactions were tested using ANOVA ( $p \leq 0.05$ ). The F-statistics were calculated using Design-Expert v8.0.6 (Stat-Ease Inc., Minneapolis, MN, USA). The data needed to fulfill several assumptions to apply the factorial ANOVA were (1) dependent variable, (2) normality, (3) homoscedasticity, and (4) no multicollinearity. X-ray fluorescence images were drawn using VESPERS graphical user interface to normalize the data, register the images, and produce multichannel visualizations [31]. X-ray fluorescence images were generated from the raw data using SigmaPlot Version 12.0 software (Systat Software Inc.). The data of X-ray fluorescence images for different treatments on day 56 were compared to observe the differences among treatments. FTIR spectra were extracted by OPUS 7.2 software (Bruker Optics). FTIR images were created by CytoSpec 2.00.01 software (Cytospec Inc.; New York, USA). Origin Pro 8.0 software (Origin lab Co.) was used for data processing and graphing. The results for FTIR were used to analyze the crop residue degradation level. The data of FTIR spectra and images for different sampling days were compared to observe the differences among sampling periods.

## 3. Results

### 3.1. Canola Yield and Significance Analyses

The effects on the canola crop yield were evaluated based on combinations of choppers and post-harvest operations, using a 2 × 3 factorial design. Canola is considered “dry” when seed moisture is at 10%. The moisture content for each sample was corrected to compensate for the moisture fluctuation under each treatment. Figure 2 shows Aftermarket \* Harrow, Aftermarket \* Tilled, OEM \* Harrow, and OEM \* Tilled had no significant difference in their canola yields, but all of them had significantly higher canola yields than the other two. Through ANOVA analyses, the tillage method was checked as the only significant main effect. As shown in Figure S4, tilled soil produced higher canola yields than harrow and check. This indicates post-harvest tillage might be the most efficient method to increase subsequent canola crop yield based on one-year data.

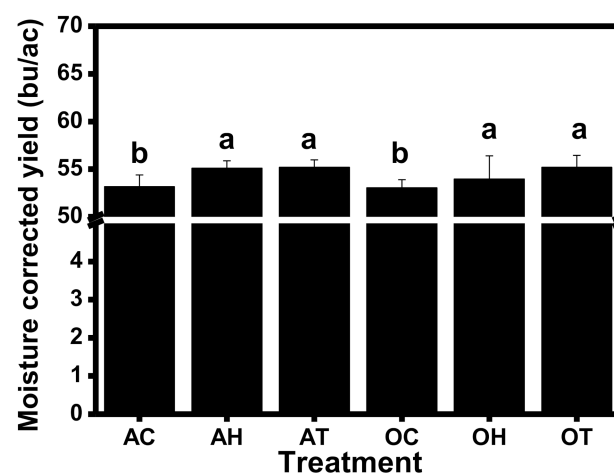


**Figure 2.** Moisture corrected yield. Note: AC: Aftermarket \* Check; AH: Aftermarket \* Harrow; AT: Aftermarket \* Tilled; OC: OEM \* Check; OH: OEM \* Harrow; OT: OEM \* Tilled. Aftermarket and OEM are different kinds of copper, indicating different crop residue treatments. Check, Harrow and Tilled indicated different kinds of tillage treatments.

### 3.2. Organic Weight of Wheat Residue

Wheat residue degradation occurred gradually in a natural soil environment. Organic matter is known to maintain soil aggregate stability. Organic weight was determined using residue samples on day 56, as shown in Figure 3. Aftermarket \* Check, OEM \* Tilled and OEM \* Check had no significant difference in organic weight per residue weight, but all of them had a significantly higher weight ratio than others. Other treatments had significantly lower weight ratios, and Aftermarket \* Harrow had the lowest ratio among all treatments. The ANOVA analysis showed no significant model in terms of weight ratio, indicating applied residue choppers and tillage methods had no significant effects on residue degradation.

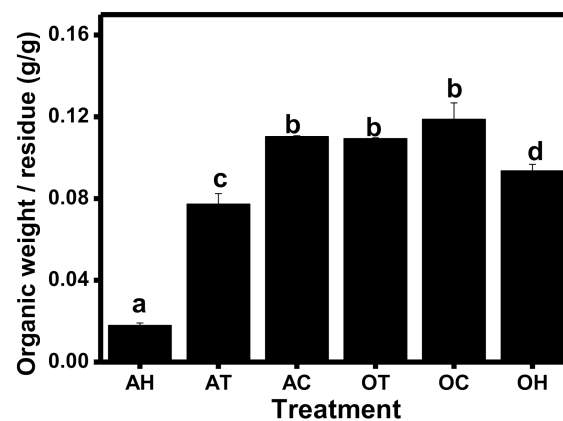


**Figure 3.** Organic weight for residue samples on day 56. Note: AC: Aftermarket \* Check; AH: Aftermarket \* Harrow; AT: Aftermarket \* Tilled; OC: OEM \* Check; OH: OEM \* Harrow; OT: OEM \* Tilled. Aftermarket and OEM are different kinds of copper, indicating different crop residue treatments. Check, Harrow and Tilled indicated different kinds of tillage treatments.

### 3.3. FTIR Analysis of Residue Decomposition

FTIR spectroscopy can be used for interpretation of the chemical structure of degraded crop residue and has become one of the most important and commonly used analytical techniques. FTIR spectra can identify the functional groups of the degraded components of crop residue. Aftermarket \* Harrow had the lowest organic weight for sampled residue on day 56 and had relatively higher crop yields. IR spectra for the corresponding residue were extracted and analyzed.

Figure 4A shows the samples from Aftermarket \* Harrow had intensive absorption in the 1600–1720  $\text{cm}^{-1}$  region. The adsorption was caused by stretching vibrations of carbonyl groups, which were formed during oxidative degradation. The occurrence of carbonyl groups indicated the depolymerization of cellulose of the crop residue, and an increase in its IR spectra intensity indicated an increase in residue oxidative degradation. There were two peaks located at the shoulder of 1700  $\text{cm}^{-1}$ . The groups at 1691  $\text{cm}^{-1}$  showed conjugation with benzene rings, and other groups at 1706  $\text{cm}^{-1}$  had no conjugation. Both structures occurred in crop residue. Figure 5A,B shows the distribution of the carbonyl group from 1685 to 1714  $\text{cm}^{-1}$  after sampling twice for Aftermarket \* Harrow. The Carbonyl group for residues sampled during the second plot visit had a higher amount than the first-time samples, which also indicates the enhanced residue oxidative degradation. Normally, with the increase of the carbonyl band, the adsorption bands in the region of C-H groups would increase. However, Figure 4B shows decreased intensity at corresponding bands of 2850 and 2918  $\text{cm}^{-1}$ . This might be because of a significant loss of organic components of the residue during the decomposition process. An increase in the spectra's intensity in the range of 1400 to 1650  $\text{cm}^{-1}$  showed a prominent change in crop residue degradation (Figure 4C). These are the primary functional groups that exist in linen, which might be targeted by soil microorganisms [32]. An increase in the peak at 1643  $\text{cm}^{-1}$  represents the

absorption of water molecules. Figure 5C,D shows the distribution of the water-molecule-related functional group at  $1643\text{ cm}^{-1}$  after sampling twice for Aftermarket \* Harrow. Residue sampled on day 56 had more water adsorption than that sampled on day 28. The increased water adsorption indicates that the structure of cellulose collapses, which causes the continuous hydrolysis of crop residue. Figure 4D shows decreased spectra intensity, particularly at  $1372$ ,  $1313$  ( $\delta\text{ CH}_2$ ),  $1160$ , and  $1105\text{ cm}^{-1}$ . This suggests crop residue degradation from high crystalline to amorphous cellulose.

The OEM \* Check treatment had the highest organic weight in the residue sampled on day 56. There were some differences in its IR spectra changes from Aftermarket \* Harrow (Figure 6). First, there were two intensive spikes centered at  $2850$  and  $2918\text{ cm}^{-1}$ . The decrease of both spectra intensities between sampling times was due to deformation vibrations of C-H groups in methyl and methylene groups ( $\text{CH}_3$ ,  $\text{CH}_2$ ,  $\text{CH}_2\text{-OH}$ ) of cellulose and lignin. Second, there was a mild intensity decrease at  $1372$ ,  $1313$  ( $\delta\text{ CH}_2$ ),  $1280$ ,  $1160$ , and  $1105\text{ cm}^{-1}$ . This mild decrease might be because of slow crop residue degradation, which was consistent with organic weight results. Aftermarket \* Check had no significant difference from OEM \* Check in moisture corrected canola yield and residue organic weight. Accordingly, the IR spectra of Aftermarket \* Check had the same trend as OEM \* Check (data not shown), suggesting the IR spectra was consistent with canola yields and residue organic weight.

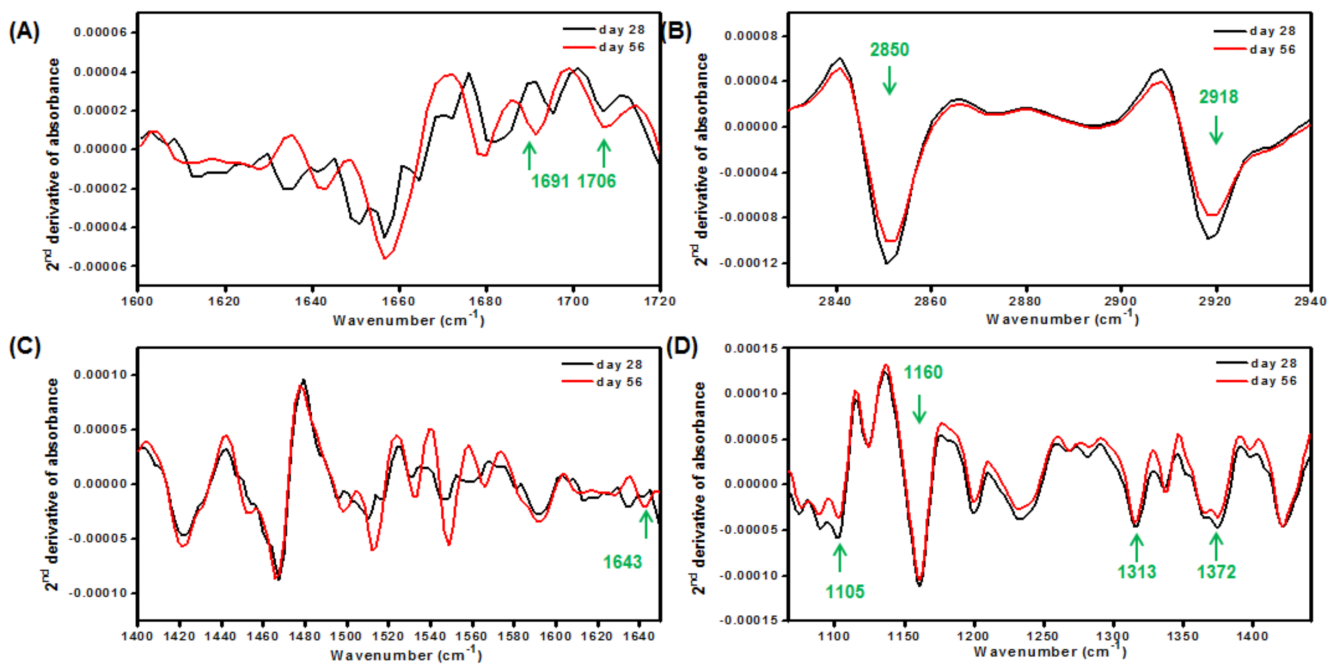


**Figure 4.** The second derivative spectrum of SR-FTIR on residue after sampling twice for Aftermarket \* Harrow. (A)  $1600\text{--}1720\text{ cm}^{-1}$ ; (B)  $2820\text{--}2940\text{ cm}^{-1}$ , (C)  $1400\text{--}1660\text{ cm}^{-1}$ , (D)  $1050\text{--}1450\text{ cm}^{-1}$ . Note: Aftermarket is one of the copper names. Harrow indicated one kind of tillage treatments.

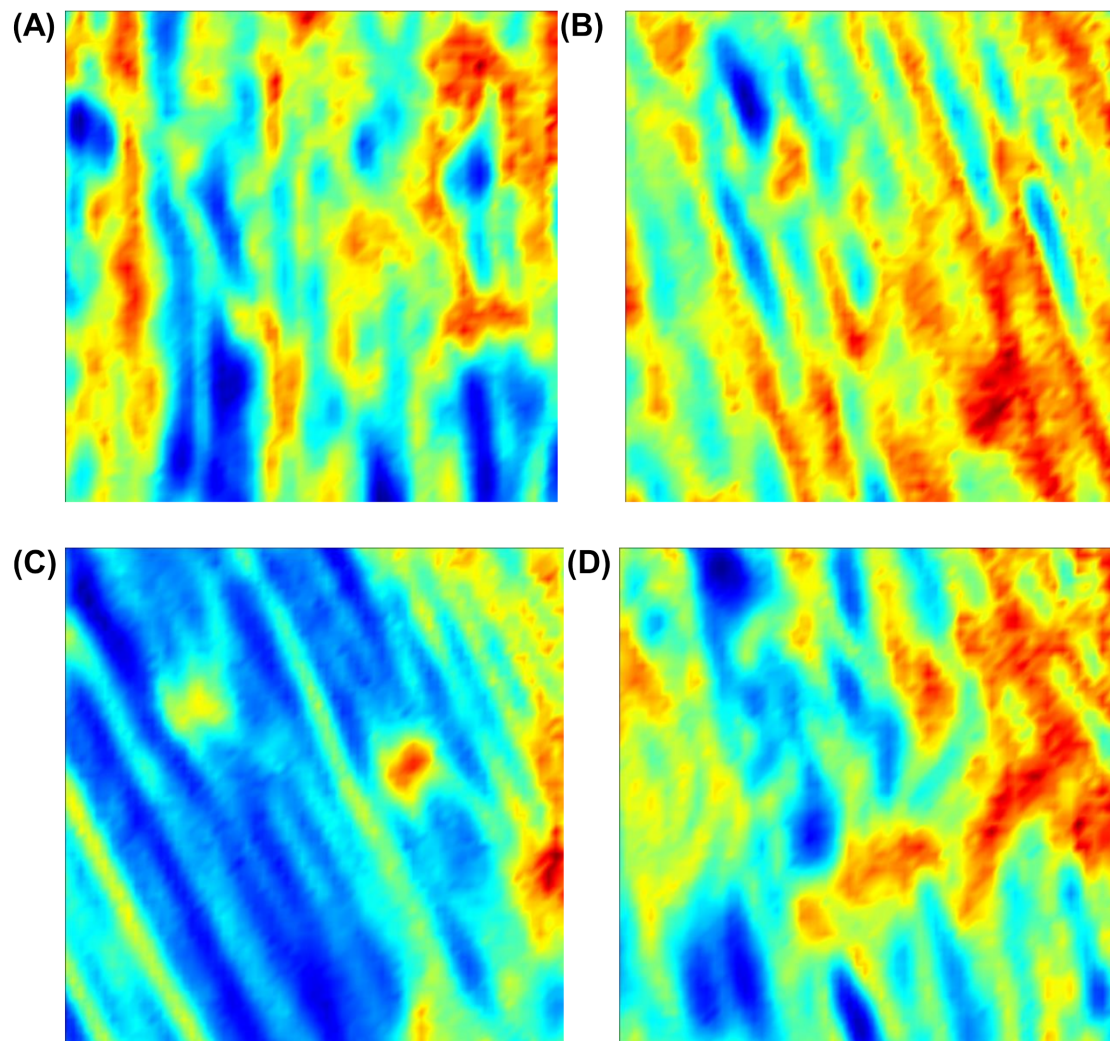


**Figure 5.** Investigation of main component distribution after sampling twice for Aftermarket \* Harrow. (A) 1685–1714  $\text{cm}^{-1}$  for 28 days post-seeding; (B) 1685–1714  $\text{cm}^{-1}$  for 56 days post-seeding; (C) 1643  $\text{cm}^{-1}$  for 28 days post-seeding; (D) 1643  $\text{cm}^{-1}$  for 56 days post-seeding. Note: Aftermarket is one of the copper names. Harrow indicated one kind of tillage treatments.

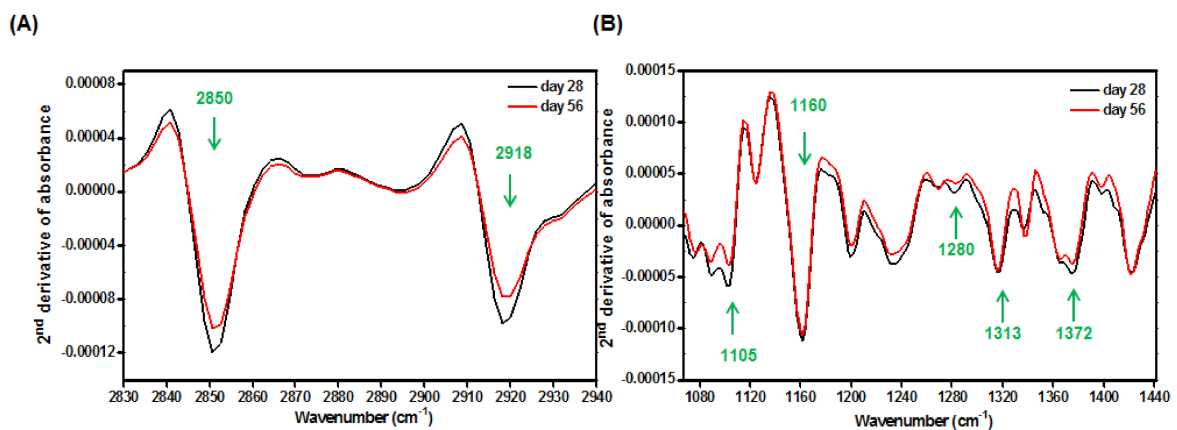


**Figure 6.** The second derivative spectrum of SR-FTIR on residue after sampling twice for OEM \* Check. (A) 2830–2940  $\text{cm}^{-1}$ ; (B) 1080–1440  $\text{cm}^{-1}$ . Note: OEM is one of the copper names. Check indicated one kind of tillage treatments.



### 3.4. XFI Analyses of Elemental Distribution

Crop residue contains large amounts of elements, such as P, K, Na, Ca, Mg, Fe, Al, and Si, and some trace elements (e.g., Zn, Cu, Ni, Be, Li, Cr, V, Co, Cd, Mn, Ga, Se, Ba, Sr, Pb, and As) [33]. These elements contributed significantly to residue degradation, because they are nutrients for soil microorganisms. There was no manual control on elements during experiment trials, and the amount of change between residue elements during both sampling events was mild. The difference in quantification was at the same order of magnitude (data not shown). Thus, there was no considerable difference in element amounts between residues under both sampling events. However, residue from different treatments but under the same sampling time had obvious changes on the same element distribution. To identify a better way to increase residue degradation efficiency, element distribution analysis for samples under Aftermarket \* Harrow and OEM \* Check on day 56 was conducted. Figure 7 shows lower amounts of almost six elements (Br, Ca, Fe, Pb, Se, and As) for Aftermarket \* Harrow treatment than that for OEM \* Check. This indicates element loss for Aftermarket \* Harrow was higher than that for OEM \* Check, which is consistent with residue organic weight results. Specifically, Br, Pb, Se, and As presented obscure higher amounts than the other two elements.

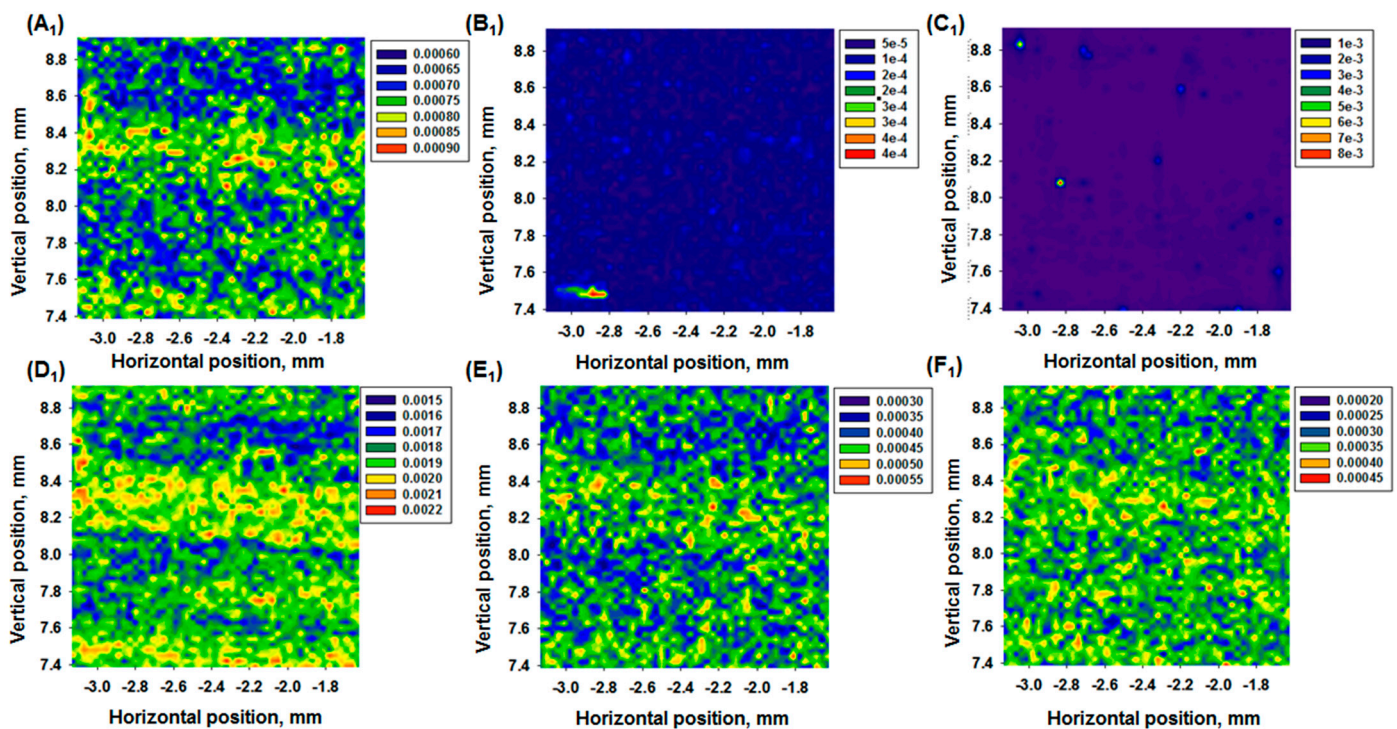
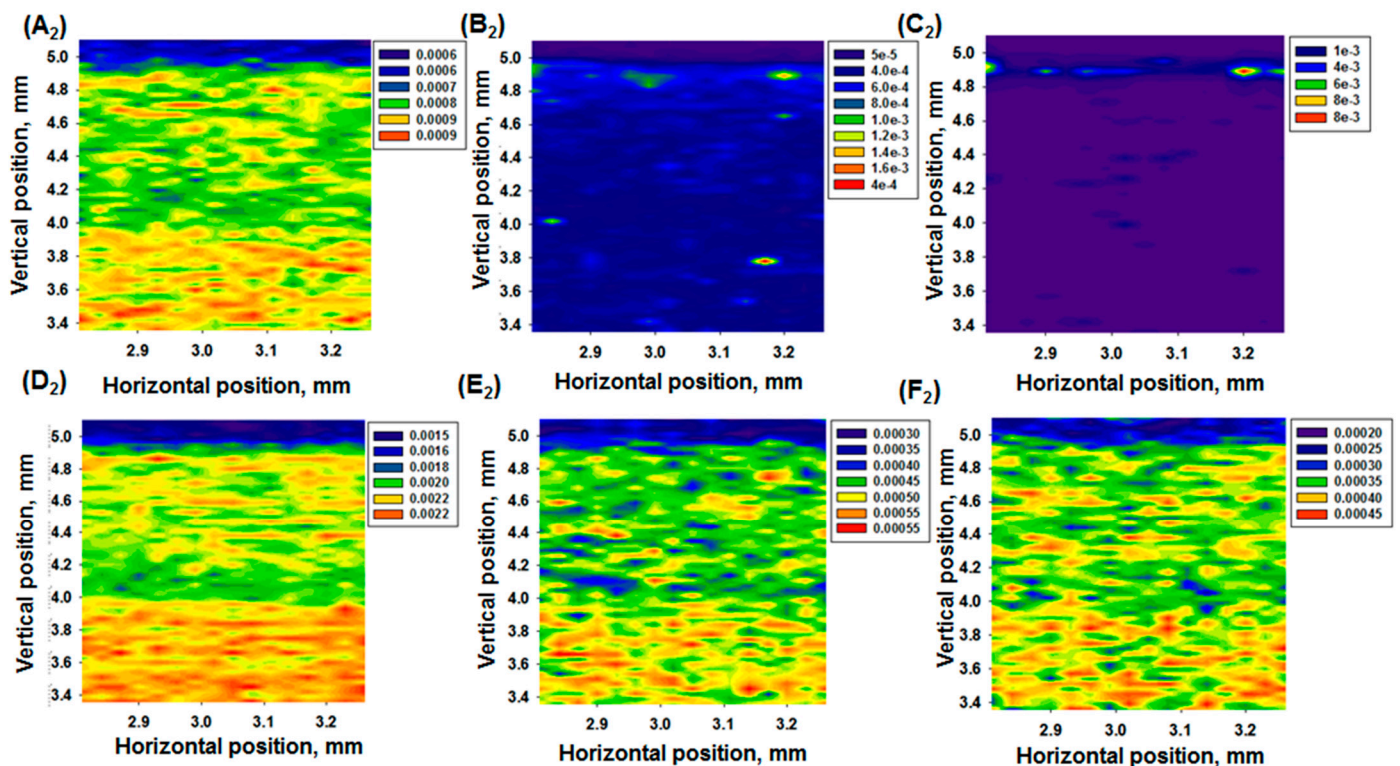


Figure 7. Cont.



**Figure 7.** Investigation of the distribution of multi-elements in residue on day 56. Aftermarket \* Harrow: (A<sub>1</sub>–F<sub>1</sub>); OEM \* Check: (A<sub>2</sub>–F<sub>2</sub>). (A<sub>1</sub>,A<sub>2</sub>) Br; (B<sub>1</sub>,B<sub>2</sub>) Ca; (C<sub>1</sub>,C<sub>2</sub>) Fe; (D<sub>1</sub>,D<sub>2</sub>) Pb; (E<sub>1</sub>,E<sub>2</sub>) Se; (F<sub>1</sub>,F<sub>2</sub>) As. Note: Aftermarket and OEM are different kinds of copper, indicating different crop residue treatments. Check and Harrow indicated different kinds of tillage treatments.

#### 4. Discussion

The purpose of this work was to evaluate residue decomposition through different residue management systems and combinations of post-harvest management practices on a high-residue wheat crop. ATR-FTIR, FTIR spectromicroscopy imaging, and SR-XFI imaging were applied to explore molecular changes and element distribution to help understand the residue degradation mechanism. An optimal management technique group was sought out to help increase agricultural production.

##### 4.1. Fundamental Knowledge of Applied Crop Residue Management Techniques

Crop residue consists of biological materials remaining on cultivated land after crop harvesting. Crop residue is an important source of organic carbon and can maintain or increase soil organic matter, providing a substrate for soil microorganisms and increasing the organic component of the soil [34]. Crop residue can provide recycled nutrients for a growing crop and better adsorb rain to decrease erosion potential [35]. Crop residues can also reduce soil erosion and improve soil moisture content [36]. Soil resources require proper management of crop residue. Crop residue decomposition can return an abundance of carbon and nutrients to the soil. Crop residue and tillage management can affect crop residue decomposition.

Crop residue can be processed through mechanical treatment using either a chopper to disperse the residue as evenly as possible or appropriate tillage operation [37]. Engine-driven choppers have been developed for chopping crop residue into small pieces. The OEM choppers and aftermarket choppers were provided by two manufacturers. OEM choppers come with the equipment, from the “original equipment manufacturer (OEM)”. The aftermarket chopper was from a different manufacturer. Tillage approaches play an important role in the manipulation of nutrient storage and organic matter release. Harrowing usually involves breaking up residue and clumps. Tilling can be an intense

process, involving mixing up the soil and going deep into the soil. In our project, the tillage tool went three inches deep and turned up the soil, making the surface black; the harrow was significantly shallower.

#### 4.2. Optimal Management Techniques for One-Year Data

Crop residue degradation can release organic matter and nutrients, which are essential requirements for growing crops. In our study, Aftermarket \* Harrow, Aftermarket \* Tilled, OEM \* Harrow, and OEM \* Tilled had a significantly higher weight ratio than Aftermarket \* Check and OEM \* Check. Residues with higher organic matter weight had lower moisture corrected canola yield. This indicates residues with a higher organic matter weight had higher organic matter content and slower degradation rate. A slower degradation rate contributed less organic matter to canola growing, leading to a lower canola yield. For example, residues from Aftermarket \* Harrow had relatively higher yields and the lowest organic weight. This indicates residues from Aftermarket \* Harrow had a higher residue degradation rate, leading to less organic matter content. The release of organic matter from residue contributed significantly to canola growth, resulting in higher canola yield. Wang's study also reported that conservation tillage showed benefits that were more prominent in combination with residue application. The benefits were found in the form of improved soil physical conditions, better water storage, and soil protection [38]. However, Verhulst found zero tillage with residue retention resulted in higher soil water content than management practices that included conventional tillage and zero tillage with residue removal [39]. Chaudhary found that *Rumex dentatus L.* exhibited higher emergence under zero tillage, with high infestation levels in rice-wheat compared to sorghum-wheat cropping systems [40]. Our study provided support on the specific combination of crop residue management and tillage treatment to achieve an increased canola yield for the Canadian agricultural industry. This ability to provide both techniques may also contribute to the global market, achieving environmental protection and permanently sustainable development at the local, regional, and global level [41]. Moreover, Aftermarket \* Tilled, OEM \* Harrow, and OEM \* Tilled had no significant difference in canola yield; however, they had significant differences in residue organic weight. This is probably because residue degradation is only one of the factors influencing crop yields. Crop residue management and tillage treatments might also cause differences in soil quality, runoff, nutrient transfer, and microorganism activity, all of which contribute to crop yields.

#### 4.3. Mechanism of Crop Residue Decomposition

Normally, residues consist mainly of cellulose, lignin, and some hemicelluloses [42]. The degradation of these main components is the residue degradation. In our study, the intensity of IR spectra of carbonyl groups increased, which was evidence of the increasing depolymerization of cellulose macromolecules. The occurrence of aromaticity has been considered as a mark of crop residue breakdown [43]. The larger the aromaticity content, the greater the degree of residue breakdown. The absorption bands in the region of C-H increased in OEM \* Check, while they decreased in Aftermarket \* Harrow. This indicates cellulose degraded in all treatments over longer periods. There was a significant loss in the cellulose of crop residue in Aftermarket \* Harrow, which corresponded to a higher residue degradation rate. Kavkler [21] had similar results in analyzing the structural changes of aged cellulosic fibers degraded by fungi. The lignin in the crop residues was probably related to cellulose in the lingo-cellulose complex, decreasing the rate of cellulose breakdown by creating a physical barrier to enzymatic attack [44,45]. Lignin was found degraded from their prominent IR spectra changes, which was mainly contributed by soil microorganisms [32]. Resistant compounds such as lignin and cellulose can be biodegraded and partially transformed into humus. Humus is the terminal of the humification process [46]. Humic substances can be taken as a major reservoir of organic carbon in soils [46] and can facilitate the uptake of organic matter by growing crops. Some specific spectra information indicated crop residue hydrolysis and supramolecular structure changes from



high crystalline to amorphous cellulose. Crystalline cellulose is normally more resistant to enzyme attack than amorphous cellulose, and it needs a much higher enzyme load for equal decomposition [47]. The transfer extent from crystalline to amorphous cellulose depends on the crop residue degradation level. OEM \* Check had milder changes than Aftermarket \* Harrow in the second derivative spectrum of SR-FTIR, indicating the former caused weaker residue degradation. IR spectra results were consistent with organic matter weight.

#### 4.4. Element Usage during Crop Residue Decomposition

Crop residue decomposition is the result of heterotrophic organism activities in the soil, mainly from soil microorganisms [48]. Soil microorganisms can break down complex organic compounds in crop residues and use major elements, such as C, N, and P, and minor elements, such as Br, Ca, Fe, Pb, Se, and As, as nutrients for their growth and make those elements available to growing crops [49]. Aftermarket \* Harrow showed lower amounts of tested elements than OEM \* Check. Among them, Br, Pb, Se, and As presented obvious differences. This indicated nutritive element transformation had been efficiently promoted under the treatment of Aftermarket \* Harrow to increase crop residue degradation and canola growing, leading to a loss of the elements remaining in crop residues. Observed from element distribution analyses, the elemental loss was accompanied by crop residue degradation. This situation is because of the availability of trace metals as micro-nutrients, which play an important role in crop residue decomposition by microorganisms [50]. Direct evidence on soil microorganism activities affecting multi-element transformation is needed in future studies. Notably, Pb and As are two heavy metals commonly found at contaminated sites. Soil microorganism activities can help remove these heavy metals simultaneously. Pb and As still need further exploration. However, residue management in combination with tillage practice can at least provide support for soil remediation to remove metal pollutants.

## 5. Conclusions

This study demonstrated the optimal treatment with the maximum canola crop production and the evaluation of wheat residue decomposition using different residue management systems and tillage treatments. An aftermarket chopper for residue treatment combined with soil harrow was identified as the optimal treatment for one-year data for our hypothesis, because it had the highest canola yields and the highest crop residue degradation rate. Crop residue degradation was attributed to cellulose/linen hydrolysis and supramolecular structure changes from high crystalline to amorphous cellulose, as revealed by FTIR spectromicroscopy. Multi-element loss accompanied by crop residue degradation was the main possible contributor to soil microorganisms revealed by SR-XFI. FTIR spectromicroscopy and SR-XFI helped explain the crop residue degradation mechanism and reveal degrading levels, indicating the reasonability and feasibility of both techniques. The findings provided suggestions for selecting efficient combinations of real-world management techniques within a western Canadian context to help maximize canola yields. This combination could probably be applied to other provinces in Canada and other countries with the ability to provide the techniques. The findings also verified the feasibility of applying FTIR spectromicroscopy and SR-XFI to help reveal the crop residue degradation mechanism. The limitation of the current study is the lack of direct evidence on soil microorganism activities affecting crop residue degradation. Further exploration of soil chemistry and element transfer through canola under specific treatment is also needed. Future work will focus on extending the experiment duration to observe the long-term effects of the applied treatments and identify an optimal treatment to achieve long-term maximum canola crop production in western Canada.

**Supplementary Materials:** The following are available online at <https://www.mdpi.com/article/10.3390/su131810459/s1>, Figure S1. Field finish in (A) harrow treatment with a 100 ft Degelman Strawmaster Pro heavy harrow; (B) tillage treatment with a 40 ft Degelman Pro-Till high-speed disc;



Figure S2. Sampling site after post-seeding on (A) day 28; (B) day 56; Figure S3. (A) The Canadian light source, (B) Bruker Vertex 70v Interferometer/Hyperion 3000 IR Microscope on Mid-IR beamline, (C) Workstation on VESPERS beamline; Figure S4. Main effect on moisture corrected yield.

**Author Contributions:** Project Administration: X.X.; Investigation: G.H.; X.X.; J.H.; Y.W.; J.Z.; Y.F.; N.W.; Methodology: X.X.; J.H.; Y.W.; J.Z.; Y.F.; N.W.; Writing Original Draft: X.X.; Conceptualization: G.H.; Review: G.H.; Supervision: G.H.; Funding Acquisition: D.H.; L.B.; Resources: D.H.; K.G.; L.B.; Visualization: K.G. All authors have read and agreed to the published version of the manuscript.

**Funding:** This research was supported by the Natural Science and Engineering Research Council of Canada (NSERC), the Canada Foundation for Innovation (CFI), and the Canada Research Chairs Program (CRC).

**Institutional Review Board Statement:** Not Applicable.

**Informed Consent Statement:** Not Applicable.

**Data Availability Statement:** Not Applicable.

**Acknowledgments:** This research was supported by the Natural Science and Engineering Research Council of Canada (NSERC), the Canada Foundation for Innovation (CFI), and the Canada Research Chairs Program (CRC). The research described in this paper was performed at the Canadian Light Source (CLS), which is supported by CFI, NSERC, University of Saskatchewan, Government of Saskatchewan, Western Economic Diversification Canada, National Research Council Canada, and Canadian Institutes of Health Research. The authors are also thankful to colleagues of the Mid Infrared Beamline and the VESPERS Beamline at CLS for providing support in the related measurement and analysis. The authors are especially grateful to Prairie Agricultural Machinery Institute for providing research data and project reports. The authors are also grateful to SaskCanola and SaskWheat for providing in-kind support and research fields. The authors are particularly grateful to the editors and the anonymous reviewers for their insightful comments and suggestions.

**Conflicts of Interest:** The authors declare no conflict of interest.

## References

1. United States Department of Agriculture. *Conservation Effects Assessment Project (CEAP)—Crop Residue Management*; United States Department of Agriculture: Washington, DC, USA, 2013.
2. Liu, J.; Zhong, F.; Niu, W.; Zhao, Y.; Su, J.; Feng, Y.; Meng, H. Effects of temperature and catalytic methods on the physicochemical properties of microwave-assisted hydrothermal products of crop residues. *J. Clean. Prod.* **2021**, *279*, 123512. [[CrossRef](#)]
3. Bentsen, N.S.; Jørgensen, J.R.; Stupak, I.; Jørgensen, U.; Taghizadeh-Toosi, A. Dynamic sustainability assessment of heat and electricity production based on agricultural crop residues in Denmark. *J. Clean. Prod.* **2019**, *213*, 491–507. [[CrossRef](#)]
4. Raza, M.H.; Abid, M.; Yan, T.; Naqvi, S.A.A.; Akhtar, S.; Faisal, M. Understanding farmers' intentions to adopt sustainable crop residue management practices: A structural equation modeling approach. *J. Clean. Prod.* **2019**, *227*, 613–623. [[CrossRef](#)]
5. Prasad, R.; Power, J. Crop residue management. In *Advances in Soil Science*; Springer: Berlin/Heidelberg, Germany, 1991; pp. 205–251.
6. Sharma, A. Performance evaluation of cultivator and its influence on various soil physical properties. *J. Pharmacog. Phytochem.* **2019**, *8*, 1688–1691.
7. Wikipedia. *Tillage*. 2020. Available online: <https://en.wikipedia.org/wiki/Tillage> (accessed on 25 July 2021).
8. Brennan, J.; Hackett, R.; McCabe, T.; Grant, J.; Fortune, R.; Forristal, P. The effect of tillage system and residue management on grain yield and nitrogen use efficiency in winter wheat in a cool Atlantic climate. *Eur. J. Agron.* **2014**, *54*, 61–69. [[CrossRef](#)]
9. Jabro, J.D.; Stevens, W.B.; Evans, R.G.; Iversen, W.M. Tillage effects on physical properties in two soils of the Northern Great Plains. *Appl. Eng. Agric.* **2009**, *25*, 337. [[CrossRef](#)]
10. Hillel, D.; Hatfield, J.L. *Encyclopedia of Soils in the Environment*; Elsevier: Amsterdam, The Netherlands, 2005; Volume 3.
11. Schomberg, H.H.; Ford, P.B.; Hargrove, W.L. Influence of crop residues on nutrient cycling and soil chemical properties. In *Managing Agricultural Residues*; Lewis Publishers, Inc.: Boca Raton, FL, USA, 1994; pp. 99–122.
12. Chen, X.; Ye, X.; Chu, W.; Olk, D.C.; Cao, X.; Schmidt-Rohr, K.; Zhang, L.; Thompson, M.L.; Mao, J.; Gao, H. Formation of Char-Like, Fused-Ring Aromatic Structures from a Nonpyrogenic Pathway during Decomposition of Wheat Straw. *J. Agric. Food Chem.* **2020**, *68*, 2607–2614. [[CrossRef](#)] [[PubMed](#)]
13. Roldán, A.; Caravaca, F.; Hernández, M.; García, C.; Sánchez-Brito, C.; Velásquez, M.; Tiscareno, M. No-tillage, crop residue additions, and legume cover cropping effects on soil quality characteristics under maize in Patzcuaro watershed (Mexico). *Soil Tillage Res.* **2003**, *72*, 65–73. [[CrossRef](#)]

14. Chávez-Romero, Y.; Navarro-Noya, Y.E.; Reynoso-Martínez, S.C.; Sarria-Guzmán, Y.; Govaerts, B.; Verhulst, N.; Dendooven, L.; Luna-Guido, M. 16S metagenomics reveals changes in the soil bacterial community driven by soil organic C, N-fertilizer and tillage-crop residue management. *Soil Tillage Res.* **2016**, *159*, 1–8. [CrossRef]
15. Bodirlau, R.; Teaca, C. Fourier transform infrared spectroscopy and thermal analysis of lignocellulose fillers treated with organic anhydrides. *Rom. J. Phys.* **2009**, *54*, 93–104.
16. Khatami, S.; Deng, Y.; Tien, M.; Hatcher, P.G. Lignin contribution to aliphatic constituents of humic acids through fungal degradation. *J. Environ. Qual.* **2019**, *48*, 1565–1570. [CrossRef]
17. Li, K.; Xing, R.; Liu, S.; Qin, Y.; Meng, X.; Li, P. Microwave-assisted degradation of chitosan for a possible use in inhibiting crop pathogenic fungi. *Int. J. Biol. Macromol.* **2012**, *51*, 767–773. [CrossRef]
18. Liang, S.; McDonald, A.G. Chemical and thermal characterization of potato peel waste and its fermentation residue as potential resources for biofuel and bioproducts production. *J. Agric. Food Chem.* **2014**, *62*, 8421–8429. [CrossRef] [PubMed]
19. Cao, Q.; Zhu, S.; Pan, N.; Zhu, Y.; Tu, H. Characterization of archaeological cotton (*G. herbaceum*) fibers from Yingpan. *Tech. Briefs Hist. Archaeol.* **2009**, *4*, 18–28.
20. Łojewska, J.; Miśkowiec, P.; Łojewski, T.; Proniewicz, L. Cellulose oxidative and hydrolytic degradation: In situ FTIR approach. *Polym. Degrad. Stabil.* **2005**, *88*, 512–520. [CrossRef]
21. Kavkler, K.; Demsar, A. Application of FTIR and Raman spectroscopy to qualitative analysis of structural changes in cellulosic fibres. *Tekstilec* **2012**, *55*, 19–31.
22. Bonnin, S.; Besson, F.; Gelhausen, M.; Chierici, S.; Roux, B. A FTIR spectroscopy evidence of the interactions between wheat germ agglutinin and N-acetylglucosamine residues. *FEBS Lett.* **1999**, *456*, 361–364. [CrossRef]
23. Canola Council of Canada. Industry Overview—Canola production. Available online: <https://www.canolacouncil.org/about-canola/industry/> (accessed on December 2020).
24. Sadik-Zada, E.R.; Loewenstein, W.; Hasanli, Y. Commodity revenues, agricultural sector and the magnitude of deindustrialization: A novel multisector perspective. *Economies* **2019**, *7*, 113. [CrossRef]
25. Sadik-Zada, E.R. Natural resources, technological progress, and economic modernization. *Rev. Dev. Econ.* **2021**, *25*, 381–404. [CrossRef]
26. Song, P.; Huang, G.; An, C.; Shen, J.; Zhang, P.; Chen, X.; Shen, J.; Yao, Y.; Zheng, R.; Sun, C. Treatment of rural domestic wastewater using multi-soil-layering systems: Performance evaluation, factorial analysis and numerical modeling. *Sci. Total Environ.* **2018**, *644*, 536–546. [CrossRef]
27. Xin, X.; Huang, G.; An, C.; Weger, H.; Cheng, G.; Shen, J.; Rosendahl, S. Analyzing the biochemical alteration of green algae during chronic exposure to triclosan based on synchrotron-based Fourier transform infrared Spectromicroscopy. *Anal. Chem.* **2019**, *91*, 7798–7806. [CrossRef] [PubMed]
28. Xin, X.; Huang, G.; An, C.; Feng, R. Interactive Toxicity of Triclosan and Nano-TiO<sub>2</sub> to Green Alga *Eremosphaera viridis* in Lake Erie: A New Perspective Based on Fourier Transform Infrared Spectromicroscopy and Synchrotron-Based X-ray Fluorescence Imaging. *Environ. Sci. Technol.* **2019**, *53*, 9884–9894. [CrossRef] [PubMed]
29. Xin, X.; Huang, G.; An, C.; Raina-Fulton, R.; Weger, H. Insights into long-term toxicity of triclosan to freshwater green algae in lake erie. *Environ. Sci. Technol.* **2019**, *53*, 2189–2198. [CrossRef]
30. Xin, X.; Huang, G.; An, C.; Lu, C.; Xiong, W. Exploring the biophysicochemical alteration of green alga *Asterococcus superbis* interactively affected by nanoparticles, triclosan and illumination. *J. Hazard. Mater.* **2020**, *398*, 122855. [CrossRef]
31. Swanston, T.; Varney, T.; Coulthard, I.; Feng, R.; Bewer, B.; Murphy, R.; Hennig, C.; Cooper, D. Elemental localization in archaeological bone using synchrotron radiation X-ray fluorescence: Identification of biogenic uptake. *J. Archaeol. Sci.* **2012**, *39*, 2409–2413. [CrossRef]
32. Mohapatra, H.; Malik, R. Effect of microorganism on flax and linen. *J. Textile Sci. Eng.* **2015**, *6*, 1–6.
33. Wang, C.; Zheng, N.; Wan, S.; Wang, J. Assessment of the modes of occurrence of trace elements in agricultural crop residues and their enrichments and bioavailability in bio-chars. *Biomass Convers. Biorefinery* **2020**, *11*, 1–13. [CrossRef]
34. Liu, X.; Herbert, S.; Hashemi, A.; Zhang, X.; Ding, G. Effects of agricultural management on soil organic matter and carbon transformation—a review. *Plant Soil Environ.* **2006**, *52*, 531. [CrossRef]
35. Blanco-Canqui, H.; Lal, R. Crop residue removal impacts on soil productivity and environmental quality. *Crit. Rev. Plant Sci.* **2009**, *28*, 139–163. [CrossRef]
36. Alliaume, F.; Rossing, W.; Tittonell, P.; Jorge, G.; Dogliotti, S. Reduced tillage and cover crops improve water capture and reduce erosion of fine textured soils in raised bed tomato systems. *Agric. Ecosyst. Environ.* **2014**, *183*, 127–137. [CrossRef]
37. Smil, V. Crop Residues: Agriculture’s Largest Harvest: Crop residues incorporate more than half of the world’s agricultural phytomass. *Bioscience* **1999**, *49*, 299–308. [CrossRef]
38. Wang, X.; Wu, H.; Dai, K.; Zhang, D.; Feng, Z.; Zhao, Q.; Wu, X.; Jin, K.; Cai, D.; Oenema, O. Tillage and crop residue effects on rainfed wheat and maize production in northern China. *Field Crops Res.* **2012**, *132*, 106–116. [CrossRef]
39. Verhulst, N.; Nelissen, V.; Jespers, N.; Haven, H.; Sayre, K.D.; Raes, D.; Deckers, J.; Govaerts, B. Soil water content, maize yield and its stability as affected by tillage and crop residue management in rainfed semi-arid highlands. *Plant Soil* **2011**, *344*, 73–85. [CrossRef]

40. Chaudhary, A.; Chhokar, R.S.; Dhanda, S.; Kaushik, P.; Kaur, S.; Poonia, T.M.; Khedwal, R.S.; Kumar, S.; Punia, S.S. Herbicide Resistance to Metsulfuron-Methyl in *Rumex dentatus* L. in North-West India and Its Management Perspectives for Sustainable Wheat Production. *Sustainability* **2021**, *13*, 6947. [[CrossRef](#)]
41. Harvanová, J. Selected aspects of integrated environmental management. *Ann. Agric. Environ. Med.* **2018**, *25*, 403–408.
42. Sun, X.; Xu, F.; Sun, R.; Fowler, P.; Baird, M. Characteristics of degraded cellulose obtained from steam-exploded wheat straw. *Carbohydr. Res.* **2005**, *340*, 97–106. [[CrossRef](#)]
43. Dignac, M.-F.; Bahri, H.; Rumpel, C.; Rasse, D.; Bardoux, G.; Balesdent, J.; Girardin, C.; Chenu, C.; Mariotti, A. Carbon-13 natural abundance as a tool to study the dynamics of lignin monomers in soil: An appraisal at the Closeaux experimental field (France). *Geoderma* **2005**, *128*, 3–17. [[CrossRef](#)]
44. Kögel-Knabner, I. The macromolecular organic composition of plant and microbial residues as inputs to soil organic matter. *Soil Biol. Biochem.* **2002**, *34*, 139–162. [[CrossRef](#)]
45. Gul, S.; Yanni, S.F.; Whalen, J.K. Lignin controls on soil ecosystem services: Implications for biotechnological advances in biofuel crops. In *Biochemistry Research Trends*; Nova Science Publishers: New York, NY, USA, 2014; pp. 375–416.
46. Tuomela, M.; Vikman, M.; Hatakka, A.; Itävaara, M. Biodegradation of lignin in a compost environment: A review. *Bioresour. Technol.* **2000**, *72*, 169–183. [[CrossRef](#)]
47. Szijártó, N.; Siika-Aho, M.; Tenkanen, M.; Alapuranen, M.; Vehmaanperä, J.; Réczey, K.; Viikari, L. Hydrolysis of amorphous and crystalline cellulose by heterologously produced cellulases of *Melanocarpus albomyces*. *J. Biotechnol.* **2008**, *136*, 140–147. [[CrossRef](#)] [[PubMed](#)]
48. Feng, Y.; Balkcom, K.S. Nutrient cycling and soil biology in row crop systems under intensive tillage. In *Soil Health and Intensification of Agroecosystems*; Elsevier: Amsterdam, The Netherlands, 2017; pp. 231–255.
49. Parr, J.; Papendick, R. Factors affecting the decomposition of crop residues by microorganisms. *Crop Residue Manag. Syst. ASA Spec. Publ.* **1978**, *31*, 101–129.
50. Demirel, B.; Scherer, P. Trace element requirements of agricultural biogas digesters during biological conversion of renewable biomass to methane. *Biomass Bioenergy* **2011**, *35*, 992–998. [[CrossRef](#)]